Proceedings of the ASME 2018 International Design Engineering Technical Conferences & Computers and Information in Engineering Conference
IDETC/CIE 2018
August 26-29, 2018, Quebec City, Canada

DETC2018-85511

DESIGN FOR ADDITIVE MANUFACTURING OF CONFORMAL COOLING CHANNELS USING THERMAL-FLUID TOPOLOGY OPTIMIZATION AND APPLICATION IN INJECTION MOLDS

Tong Wu **Andres Tovar**
Department of Mechanical and Energy Engineering
Purdue School of Engineering and Technology
Indiana University-Purdue University Indianapolis
Indianapolis, Indiana, USA
wu616@purdue.edu, tovara@iupui.edu

ABSTRACT

Additive manufacturing allows the fabrication parts and tools of high complexity. This capability challenges traditional guidelines in the design of conformal cooling systems in heat exchangers, injection molds, and other parts and tools. Innovative design methods, such as network-based approaches, lattice structures, and structural topology optimization have been used to generate complex and highly efficient cooling systems; however, methods that incorporate coupled thermal and fluid analysis remain scarce. This paper introduces a coupled thermal-fluid topology optimization algorithm for the design of conformal cooling channels. With this method, the channel position problem is replaced to a material distribution problem. The material distribution directly depends on the effect of flow resistance, heat conduction, as well as forced and natural convection. The problem is formulated based on a coupling of Navier-Stokes equations and convection-diffusion equation. The problem is solved by gradient-based optimization after analytical sensitivity derived using the adjoint method. The algorithm leads a two -dimensional conceptual design having optimal heat transfer and balanced flow. The conceptual design is converted to three-dimensional channels and mapped to a morphological surface conformal to the injected part. The method is applied to design an optimal conformal cooling for a real three dimensional injection mold. The feasibility of the final designs is verified through simulations. The final designs can be exported as both three-dimensional graphic and surface mesh CAD format, bringing the manufacture department the convenience to run the tool path for final fitting.

Keywords: thermal-fluid coupled topology optimization; conformal cooling; injection mold; additive manufacturing.

1 Introduction

Additive manufacturing allows the fabrication parts and tools of high complexity, challenging traditional design guidelines of conformal cooling systems in heat exchangers, injection molds, and other parts of and tooling. Particularly, in injection molding process, careful control of surface temperature and heat transfer rate is required to improve quality and increase the efficiency of production. Additive manufacturing (AM) enables several innovative design approaches that intricate cooling system in mold inserts, conformal the shape of plastic inject part, offering significant reduction of cost savings [1].

1.1 Advanced cooling system design for injection molds

These advanced design approaches can be categorized into Morphological Surfaces (MS) based cooling network, lattice cooling (LC) layer and optimized conformal cooling system. A Morphological Surface (MS) is defined as an expand offset surface of the injected part, in which the cooling channels are re-

This is the author's manuscript of the article published in final edited form as:
Wu, T., & Tovar, A. (2018, August). Design for Additive Manufacturing of Conformal Cooling Channels Using Thermal-Fluid Topology Optimization and Application in Injection Molds. In ASME 2018 International Design Engineering Technical Conferences and Computers and Information in Engineering Conference (pp. V02BT03A007-V02BT03A007). American Society of Mechanical Engineers. https://doi.org/10.1115/DETC2018-85511

stricted to be positioned [2]. Since the designed channels are located on the surface conformal to the heat source, a better uniformity of temperature field can be obtained. Agazzi et al. positioned the cooling channels referred to the isothermal contours after thermal finite element simulation without cooling, then use the trail-and-error method to find the satisfied design (Fig. 1(a)) [3]. Wang et al. used a Centroid Voronoi Diagram to generate a complex flow network, looking like capillary network in body, thoroughly covered the entire morphology surface [4] (Fig. 1(b)). Simulations have shown that, when cooling flow successfully pass through this flow network, this design has reducing cooling time, improved temperature uniformity and reduced volume shrinkage. However, in this design, all pipes in the flow network have nearly the same hydraulic radius, which makes it difficult to ensure adequate flow rates in the pipes far from the inlet and outlet.

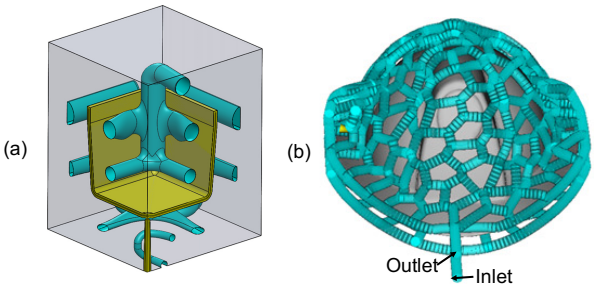

FIGURE 1. (a) CONFORMAL COOLING DESIGNS POSITIONED ON MORPHOLOGICAL SURFACES [3]. (b) A CENTROID VORONOI DIAGRAM BASED FLOW NETWORK LOCATED ON MORPHOLOGICAL SURFACES [4].

Implementing cooling layers with lattice structure (LC) to cooling down injection molds was proposed by Au and Yu, and the effectiveness was demonstrated by implementing thermal and mechanical simulations [5]. Hardley and Kevin design and test lattice cooling with easy-to-build support lattices for efficient and balanced heat transfer (Fig. 2) [6]. Wu et al. propose to deviating the porosity distribution of the lattice cells to obtain an optimal LC structure [7]. Although it's known that lattice cooling provides superior structure whilst improving heat transfer in some industries [8], it is still not widely applicable in plastic injection industry, for it is difficult to clean up the clogging inside the lattice structure after a short service period.

Compared to MS and LC cooling systems, optimized conformal cooling systems that improve heat transfer of the original design are feasible and have been extensively studied [9, 10]. In these studies, conformal cooling systems were optimized in terms of parametrized geometric control points, and their optimal shapes were obtained through parametric optimization or surrogate models. Unfortunately, the optimal design obtained by these studies do not permit adding new channels or modifying connectivity of channels during the optimization process. Our research has introduced thermal-fluid coupled topology optimization to refine and amplify conformal cooling designs.

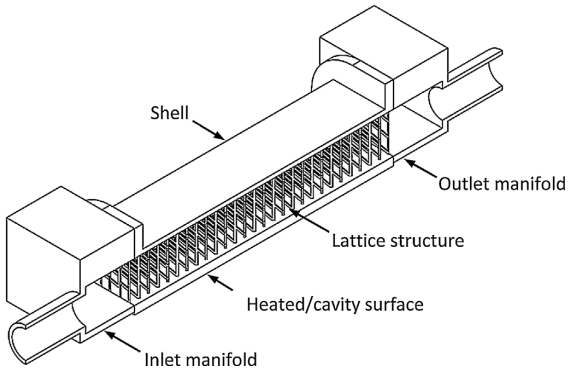

FIGURE 2. A CONCEPTUAL DESIGN OF LATTICE COOLING [6].

1.2 Thermal-fluid topology optimization

As a particularly useful finite element analysis based design approach, topology optimization is the replacement of a structural optimization problem with material distribution problem, brings a high degree of geometric freedom for the conceptual design. The proposed method fully combines thermal and fluid topology optimization to obtain an optimal cooling pipe system in the heated design domain. Expansive studies can be found for topology optimization associated with thermal conduction [11–14]. Natural heat convection has been included in [15–17]. So far, large scale three-dimensional heat sink cooled by thermal conduction and natural convection obtained from topology optimization is available for experimental tests [18, 19]. Forced convection has also been addressed by introducing surrogate material interpolation models [7, 20, 21]. On the other hand, many studies aim to find flow passages having minimized energy loss using topology optimization [22–28]. In these researches, the optimal designs are mainly derived from Stokes flow [22, 23] and laminar flow [25, 26]. Topology optimization based on turbulent flow model is still a new research area, in which only a few of recent studies have been performed [27, 28].

In a thermal-fluid coupled system, thermal and fluid finite element analysis are dependent. In Koga et al. [29] and Dede's work [21, 30], velocity field of the fluid flow derived from Stokes flow model is introduced to the thermal model to determine forced convection, and the material distribution directly depends on flow resistance. In topology optimization, two objectives associated with thermal and fluid performance are aggregated through weighting coefficients, to formulate a multi-objective

function. Further, this appraoch has been accomplished in detail, leaded an improvement of optimality [31–33]. In addition, in these studies, the fluid model has been broaden from a Stokes flow to Laminar flow model. However, these studies only consider the heat transfer that is locally dependent on the flow field and evaluated quantitatively on the fluid-solid boundary [32]. Besides,the results occasionally represented an unbalanced flow, makes no sufficient flow rate through certain areas of a channel, thus resulting in limited and non uniform heat transfer.

The proposed method aims to evaluate and optimize comprehensive heat transfer performance of the entire design domain. In the proposed method, material distribution is directly affected by flow resistance, heat conduction, as well as natural and forced convection. In addition, to specify the cooling uniformity demand for an injection mold, the flow balance of the cooling system is calibrated. The consequential conceptual design is transferred to a Computer-aided Design (CAD) format, and mapped to a morphological surface that conformal to the injected part. For the fluid model, to reduce the computational cost, a laminar flow is assumed in optimization procedure in which the finite element model is frequently called, and the feasibility of final three dimensional design is verified in thermal-fluid finite element analysis using a turbulent model. Final three-dimensional designs can be exported as both 3D graphic and surface mesh format, brings the manufacture department the convenience to run the tool path for final fitting.

The paper is organized as follows. The thermal-fluid model with respect to the proposed algorithm is described in Section 2, while coupled thermal-fluid topology optimization problem and the associated sensitivity analysis and post-processing are posed in Section 3. In Section 4, the method is applied to the optimal design of conformal cooling system of an injection mold.

2 Derivation of the thermal-fluid model

The governing equations and their discretized form of thermal-fluid finite analysis required in the proposed method, including fluid-flow model and heat transfer model are briefly described in this section. The details of these methods are illustrated in [20, 23, 29].

2.1 Fluid-flow model

A fluid finite element model is based on Navier-Stokes equations. A steady state Navier-Stokes equations without fluid body force can be described by momentum and continuity equations are presented as follows:

$$\begin{aligned} &\rho\left(\boldsymbol{u}\cdot\boldsymbol{\nabla}\right)\boldsymbol{u} = -\boldsymbol{\nabla}p + \eta\nabla^2\boldsymbol{u} - \alpha(\theta)\boldsymbol{u} \\ &\boldsymbol{\nabla}\cdot\boldsymbol{u} = 0, \end{aligned} \tag{1}$$

where ρ is the fluid density, $\boldsymbol{u}$ is the velocity field, p is the pressure field, η is the fluid dynamic viscosity. $\alpha(\theta)$ is interpolation function of Brinkman Stiffness:

$$\alpha(\theta_e) = \theta_0\left(\theta_{\min} + (1-\theta_{\min})\frac{p_b(1-\theta_e)}{p_b+\theta_e}\right), \tag{2}$$

where θ_e is the proportion of fluid in an element, p_b is a positive penalty parameter used for tuning the function shape of $\alpha(\theta_e)$ (Fig. 3). This term can be interpreted as a large damping term that stops flow, which ensures the velocity in the solid domain ($\alpha(\theta_e)$=0) vanishes. θ_0 is a coefficient to amplify this damping effect.

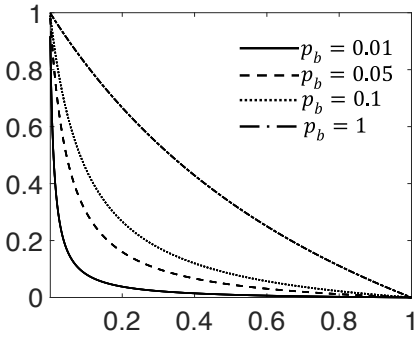

FIGURE 3. THE SHAPE OF INTERPOLATION FUNCTION $\alpha(\theta_e)$ IS INFLUENCED BY PENALTY PARAMETER p_b.

By applying Galerkin method and Green identity, Eq. (1) can be discretized to

$$\underbrace{\begin{bmatrix}\mathbf{K} & -\mathbf{G}^\intercal \\ -\mathbf{G} & \mathbf{0}\end{bmatrix}}_{\mathbf{K}_g}\underbrace{\begin{bmatrix}\mathbf{u}\\ \mathbf{p}\end{bmatrix}}_{\mathbf{U}} = \underbrace{\begin{bmatrix}\mathbf{f}\\ \mathbf{0}\end{bmatrix}}_{\mathbf{F}}, \tag{3}$$

where $\mathbf{u}$, $\mathbf{p}$ and $\mathbf{f}$ are nodal velocity, pressure and force, respectively. In a two dimensional problem, each node contains two directions of velocities: $\mathbf{u}_e$=$\{\mathbf{u}_e^x, \mathbf{u}_e^y\}$. The matrix $\mathbf{K}$ is constructed as

$$\mathbf{K} = \mathbf{K}_s + \mathbf{K}_b + \mathbf{K}_a. \tag{4}$$

$\mathbf{K}$ can be considered as a union of the matrices with respect to two directions of velocities $\mathbf{K}$=$\{\mathbf{K}^x, \mathbf{K}^y\}$. In this equation, the stiffness matrix of Stokes flow

$$\mathbf{K}_s = \sum_{e=1}^{n_e}\int_{V_e}\nabla\mathbf{N}_\mathbf{u}{}^\intercal\mathbf{I}_0\nabla\mathbf{N}_\mathbf{u}\mathrm{d}V_e, \tag{5}$$

where $\mathbf{N_u}$ is the matrix containing shape functions of the elemental velocity, and

$$\mathbf{I}_0 = \begin{bmatrix} 2\ 0\ 0 \\ 0\ 2\ 0 \\ 0\ 0\ 1 \end{bmatrix}. \tag{6}$$

for a two dimensional element. $\mathbf{K}_b$ is the Brinkman damping matrix, which can be considered as a union of matrices with respect to two directions of velocities: $\mathbf{K}_b$=$\{\mathbf{K}_b^x, \mathbf{K}_b^y\}$. For both x and y directions, the matrix is constructed as:

$$\mathbf{K}_b^x = \mathbf{K}_b^y = \sum_{e=1}^{n_e} \int_{V_e} \alpha(\theta_e) \mathbf{N_u}^\intercal \mathbf{N_u} \mathrm{d}V_e, \tag{7}$$

$\mathbf{K}_a$ is the advection matrix, which can be considered as a union of matrices with respect to two directions of velocities: $\mathbf{K}_a$=$\{\mathbf{K}_a^x, \mathbf{K}_a^y\}$. For both x and y directions, the matrix is constructed as:

$$\mathbf{K}_a^x = \mathbf{K}_a^y = \sum_{e=1}^{n_e} \int_{V_e} \left(\underbrace{\mathbf{N_u}^\intercal \mathbf{N_u} \mathbf{u}_e^x \nabla \mathbf{N_u}_{,x}}_{\mathbf{K}_a^{xx} \ and \ \mathbf{K}_a^{yx}} + \underbrace{\mathbf{N_u}^\intercal \mathbf{N_u} \mathbf{u}_e^y \nabla \mathbf{N_u}_{,y}}_{\mathbf{K}_a^{xy} \ and \ \mathbf{K}_a^{yy}} \right) \mathrm{d}V_e. \tag{8}$$

$\mathbf{G}$ is the coupling matrix of the pressure and velocity of x and y directions : $\mathbf{G}$=$\{\mathbf{G}^x, \mathbf{G}^y\}$, where

$$\mathbf{G}^x = \sum_{e=1}^{n_e} \int_{V_e} \nabla \mathbf{N_u}_{,x}^\intercal \mathbf{N_p} \mathrm{d}V_e, \tag{9}$$

and

$$\mathbf{G}^y = \sum_{e=1}^{n_e} \int_{V_e} \nabla \mathbf{N_u}_{,y}^\intercal \mathbf{N_p} \mathrm{d}V_e. \tag{10}$$

Since nodal velocity is presented in both $\mathbf{K}_g$ and $\mathbf{U}$ of Eq. (3), iterative method is required to solve this equation. In this study, a Picard iterative method is used, the details of this method is presented in [34].

2.2 Heat transfer model

On the other hand, a steady state heat transfer equation (convection-diffusion equation) is also required in a coupled thermal-fluid finite element analysis:

$$h_2(\theta) \left[\boldsymbol{u}(\theta) \cdot \boldsymbol{\nabla} \right] T = k(\theta) \boldsymbol{\nabla}^2 T - h_1(\theta) T. \tag{11}$$

where $\boldsymbol{u}(\theta)$ is the fluid velocity derived from the fluid problem. $k(\theta)$ and $h_1(\theta)$ and $h_2(\theta)$ are material interpolation functions of heat conduction, natural and forced convection, respectively:

$$\begin{aligned} k(\theta_e) &= k^0 \left(\theta_{\min} + (1-\theta_{\min})(1-\theta_e)^{p_c}\right) \\ h_1(\theta_e) &= h_1^0 \left(\theta_{\min} + (1-\theta_{\min})\theta_e^{p_n}\right) \\ h_2(\theta_e) &= h_2^0 \left(\theta_{\min} + (1-\theta_{\min})\theta_e^{p_v}\right). \end{aligned} \tag{12}$$

These interpolation schemes indicate, in an element, the heat conduction is mainly applied to the solid phase and the fluid phase is dominated by convection. p_c, p_n and p_v are the penalty parameters associated with heat conduction, natural convection and forced convection, respectively. A zero value of these penalty parameters implies that the associated heat transfer in an element is independent of proportion of fluid. k^0 is the heat conductivity of a pure solid element, h_1^0 and h_2^0 are the natural and forced convection coefficient of a fluid element.

With the application of Galerkin method and Green identity, Eq. (11) can be discretized to

$$\mathbf{K}_t \mathbf{T} = \mathbf{q}, \tag{13}$$

where $\mathbf{q}$ is the boundary heat flux, and $\mathbf{T}$ is the vector of nodal temperatures. The matrix $\mathbf{K}_t$ is constructed as

$$\mathbf{K}_t = \mathbf{K}_c + \mathbf{K}_n + \mathbf{K}_v. \tag{14}$$

In this equation, the stiffness matrix of thermal conduction is

$$\mathbf{K}_c = \sum_{e=1}^{n_e} \int_{V_e} k(\theta_e) \nabla \mathbf{N_T}^\intercal \boldsymbol{\kappa} \nabla \mathbf{N_T} \mathrm{d}V_e, \tag{15}$$

where $\mathbf{N_T}$ is the matrix containing shape functions of the elemental temperature, and

$$\boldsymbol{\kappa} = \begin{bmatrix} 1\ 0 \\ 0\ 1 \end{bmatrix}. \tag{16}$$

for a two dimensional element. $\mathbf{K}_n$ is the natural convection matrix, which is constructed as

$$\mathbf{K}_n = \sum_{e=1}^{n_e} \int_{V_e} h_1(\theta_e) \mathbf{N_T}^\intercal \mathbf{N_T} \mathrm{d}V_e. \tag{17}$$

$\mathbf{K}_v$ is the convection matrix, which is constructed as:

$$\mathbf{K}_v = \sum_{e=1}^{n_e} \int_{V_e} h_2(\theta_e) \Bigg(\underbrace{\mathbf{N_u}^\intercal \mathbf{N_u} \mathbf{u}_e^x \nabla \mathbf{N_T}_{,x}}_{\mathbf{N}_v^x} + \underbrace{\mathbf{N_u}^\intercal \mathbf{N_u} \mathbf{u}_e^y \nabla \mathbf{N_T}_{,y}}_{\mathbf{N}_v^y} \Bigg) \mathrm{d}V_e. \tag{18}$$

3 Thermal-fluid topology optimization method

In this section, the problem statement is defined. The schematic figure of the design domain in this study is shown in Fig. 4. The proposed method aims to search for the optimal topology in the design domain Ω, with prescribed heat source q, inflow and outflow locations (Γ_{inflow} and $\Gamma_{outflow}$), as well as the inflow and outflow properties such as velocity v, temperature T and pressure p.

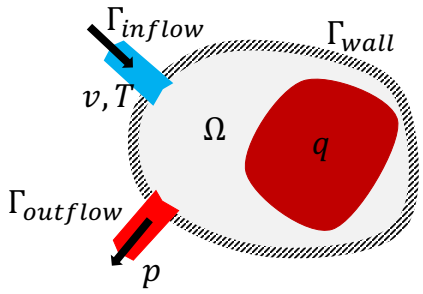

FIGURE 4. PROBLEM SETTING OF THE PROPOSED TOPOLOGY OPTIMIZATION ALGORITHM.

To clarify this method, the fluid, thermal and coupled thermal-fluid topology optimization are sequentially represented. Further, the associated sensitivity analysis and post processing of the conceptual design are described,

3.1 Problem statement of the conceptual design

In all of the three problems, a prescribed amount of fluid in the design domain

$$\sum_{e=1}^{n_e} v_e \theta_e \leq V, \tag{19}$$

is allowed while optimizing the objectives. A well known objective of a Navier-Stokes flow topology optimization is to minimize the energy dissipation in the system:

$$Q_1 = -\mathbf{f}^\intercal \mathbf{u}. \tag{20}$$

In addition, a global gradient constraint

$$R(\boldsymbol{\theta}) = \sum_{e=1}^{n_e} \nabla \theta_e{}^\intercal \nabla \theta_e, \tag{21}$$

can be included to the objective to control the complexity of the geometry, where $\boldsymbol{\theta}$ the vector contains elemental relative solid phase densities in the design domain. Further, the finite element analysis Eq. (3) is required as a constraint. Finally, the optimization problem of a fluid problem is stated as:

$$\begin{aligned} \text{find} \quad & \boldsymbol{\theta}_1^* \in \mathbb{R}^{n_e} \\ \min \quad & Q_1 = -\mathbf{f}^\intercal \mathbf{u} + \gamma_1 R(\boldsymbol{\theta}) \\ \text{s.t.} \quad & \begin{bmatrix} \mathbf{K} & -\mathbf{G}^\intercal \\ -\mathbf{G} & \mathbf{0} \end{bmatrix} \begin{bmatrix} \mathbf{u} \\ \mathbf{p} \end{bmatrix} = \begin{bmatrix} \mathbf{f} \\ \mathbf{0} \end{bmatrix} \\ & \sum_{e=1}^{n_e} v_e \theta_e \leq V, \end{aligned} \tag{22}$$

For a thermal problem, the thermal compliance, which is widely used to handle heat transfer problem, is adopted as the objective function:

$$Q_2 = \mathbf{q}^\intercal \mathbf{T}, \tag{23}$$

Minimizing this objective under constant heat source leads to a minimization of the temperature at constant heat flux boundary. Additionally, the finite element analysis in Eq. (13) is required as a constraint. Thus, the optimization of a thermal problem is stated as:

$$\begin{aligned} \text{find} \quad & \boldsymbol{\theta}_2^* \in \mathbb{R}^{n_e} \\ \min \quad & Q_2 = \mathbf{q}^\intercal \mathbf{T} + \gamma_2 R(\boldsymbol{\theta}) \\ \text{s.t.} \quad & \mathbf{K}_t \mathbf{T} = \mathbf{q} \\ & \sum_{e=1}^{n_e} v_e \theta_e \leq V, \end{aligned} \tag{24}$$

In the proposed thermal-fluid coupled problem, thermal compliance is formulated as the objective, both fluid and thermal finite element analysis are needed as constraints. The optimiza-

tion of a thermal-fluid problem is stated as:

$$\begin{aligned} \text{find} \quad & \boldsymbol{\theta}_2^{c*} \in \mathbb{R}^{n_e} \\ \text{min} \quad & Q_2^c = \mathbf{q}^\intercal \mathbf{T} + \gamma_2^c R(\boldsymbol{\theta}) \\ \text{s.t.} \quad & \begin{bmatrix} \mathbf{K} & -\mathbf{G}^\intercal \\ -\mathbf{G} & \mathbf{0} \end{bmatrix} \begin{bmatrix} \mathbf{u} \\ \mathbf{p} \end{bmatrix} = \begin{bmatrix} \mathbf{f} \\ \mathbf{0} \end{bmatrix} \\ & \mathbf{K}_t(\mathbf{u})\,\mathbf{T} = \mathbf{q} \\ & \sum_{e=1}^{n_e} v_e \theta_e \leq V. \end{aligned} \tag{25}$$

3.2 Sensitivity analysis

The sensitivities of these three problems can be derived using the adjoint method. For a fluid problem, to begin with, a null term is added to the original expression (without the additional gradient constraint):

$$Q_1 = -\mathbf{f}^\intercal \mathbf{u} + \boldsymbol{\lambda}_f^\intercal (\mathbf{K}_g \mathbf{U} - \mathbf{F}) \tag{26}$$

The sensitivity of this augmented expression is

$$\frac{\partial Q_1}{\partial \theta_e} = -\mathbf{f}^\intercal \frac{\partial \boldsymbol{u}}{\partial \theta_e} + \boldsymbol{\lambda}_f^\intercal \left(\frac{\partial \mathbf{K}_b}{\partial \theta_e}\mathbf{u} + \frac{\partial \mathbf{K}_a}{\partial \mathbf{u}} \frac{\partial \mathbf{u}}{\partial \theta_e}\mathbf{u} + \mathbf{K}\frac{\partial \mathbf{u}}{\partial \theta_e} \right) \tag{27}$$

To remove the field of sensitivity of $\frac{\partial \mathbf{u}}{\partial \theta_e}$, the following expression should be zero:

$$\left(\boldsymbol{\lambda}_f^\intercal \left(\frac{\partial \mathbf{K}_a}{\partial \mathbf{u}}\mathbf{u} + \mathbf{K} \right) - \mathbf{f}^\intercal \right) \frac{\partial \mathbf{u}}{\partial \theta_e} = \mathbf{0}, \tag{28}$$

The adjoint vector $\boldsymbol{\lambda}_f$ can be obtained by solving Eq. (28), therefore the sensitivity of a fluid problem can be written as

$$\frac{\partial Q_1}{\partial \theta_e} = \boldsymbol{\lambda}_f^\intercal \frac{\partial \mathbf{K}_b}{\partial \theta_e}\mathbf{u}. \tag{29}$$

Similarly, the sensitivity of a thermal problem can be derived, started by adding a null term to the original expression (without the additional gradient constraint):

$$Q_2 = \mathbf{q}^\intercal \mathbf{T} + \boldsymbol{\lambda}_t^\intercal (\mathbf{K}_t \mathbf{T} - \mathbf{q}). \tag{30}$$

The sensitivity of this augmented expression is

$$\frac{\partial Q_2}{\partial \theta_e} = \mathbf{q}^\intercal \frac{\partial \mathbf{T}}{\partial \theta_e} + \boldsymbol{\lambda}_t^\intercal \left(\frac{\partial \mathbf{K}_t}{\partial \theta_e}\mathbf{T} + \mathbf{K}_t \frac{\partial \mathbf{T}}{\partial \theta_e} \right). \tag{31}$$

To remove the field of sensitivity of $\frac{\partial \mathbf{T}}{\partial \theta_e}$, the following expression should be zero:

$$\left(\boldsymbol{\lambda}_t^\intercal \mathbf{K}_t + \mathbf{q}^\intercal \right) \frac{\partial \mathbf{T}}{\partial \theta_e} = \mathbf{0}. \tag{32}$$

The adjoint vector $\boldsymbol{\lambda}_t$ can be obtained by solving Eq. (32), so that the sensitivity of a fluid problem can be written as

$$\frac{\partial Q_2}{\partial \theta_e} = \boldsymbol{\lambda}_t^\intercal \frac{\partial \mathbf{K}_t}{\partial \theta_e}\mathbf{T}. \tag{33}$$

For the proposed thermal-fluid coupled topology optimization, to begin with, two null terms are added to the original expression (without the additional gradient constraint)

$$Q_2^c = \mathbf{q}^\intercal \mathbf{T} + + \boldsymbol{\lambda}_f^\intercal (\mathbf{K}_g \mathbf{U} - \mathbf{F}) + \boldsymbol{\lambda}_t^\intercal (\mathbf{K}_t \mathbf{T} - \mathbf{q}). \tag{34}$$

The sensitivity of this augmented expression is

$$\begin{aligned} \frac{\partial Q_2}{\partial \theta_e} = {} & \mathbf{q}^\intercal \frac{\partial \mathbf{T}}{\partial \theta_e} + \boldsymbol{\lambda}_f^\intercal \left(\left(\frac{\partial \mathbf{K}_b}{\partial \theta_e} + \frac{\partial \mathbf{K}_a}{\partial \mathbf{u}} \frac{\partial \mathbf{u}}{\partial \theta_e} \right) \mathbf{u} + \mathbf{K} \frac{\partial \mathbf{u}}{\partial \theta_e} \right) \\ & + \boldsymbol{\lambda}_t^\intercal \left(\left(\frac{\partial \mathbf{K}_c}{\partial \theta_e} + \frac{\partial \mathbf{K}_n}{\partial \theta_e} + \frac{\partial \mathbf{K}_v}{\partial \theta_e} \right) \mathbf{T} + \mathbf{K}_t \frac{\partial \mathbf{T}}{\partial \theta_e} \right). \end{aligned} \tag{35}$$

To remove the field of sensitivity of $\frac{\partial \mathbf{T}}{\partial \theta_e}$ and $\frac{\partial \mathbf{u}}{\partial \theta_e}$ the following expression should be zero:

$$\begin{aligned} & \left(\mathbf{q}^\intercal + \boldsymbol{\lambda}_t^\intercal \mathbf{K}_t \right) \frac{\partial \mathbf{T}}{\partial \theta_e} = \mathbf{0} \\ & \boldsymbol{\lambda}_f^\intercal \mathbf{K} \frac{\partial \mathbf{T}}{\partial \theta_e} = \mathbf{0}. \end{aligned} \tag{36}$$

The adjoint vectors $\boldsymbol{\lambda}_t$ and $\boldsymbol{\lambda}_f$ can be obtained by solving Eq. (33). It is straightforward that $\boldsymbol{\lambda}_f = \mathbf{0}$. Therefore, the sensitivity of a fluid problem can be written as

$$\boldsymbol{\lambda}_t^\intercal \left(\frac{\partial \mathbf{K}_c}{\partial \theta_e} + \frac{\partial \mathbf{K}_n}{\partial \theta_e} + \frac{\partial \mathbf{K}_v}{\partial \theta_e} \right) \mathbf{T}. \tag{37}$$

The sensitivities can be employed to the topology optimization problems, and a gradient-based sequential convex programming algorithm called Method of Moving Asymptotes (MMA) solver [35] is used to solve the constrained optimization problem.

3.3 Flow balance and final design

To achieve the flow balance in the system, an additional optimization problem is formulated. In this problem statement, the resulting topology derived from Eq. (25) is utilized. In the conceptual design obtained through Eq. (25), a section Γ_i contains number n of flow channels is selected. Same velocity $u_1^i = \cdots u_n^i$ is distributed on each of the pipe sections $\mathbf{d}_1^i = \cdots \mathbf{d}_n^i$. With this new boundary condition, a fluid topology optimization is formulated:

$$
\begin{aligned}
\text{given} \quad & \boldsymbol{\theta}_2^{c*} \in \mathbb{R}^{n_e} \\
& \boldsymbol{u}_1^i = \boldsymbol{u}_2^i = \cdots \boldsymbol{u}_n^i \\
& \in \{\boldsymbol{d}_1^i = \boldsymbol{d}_2^i = \cdots \boldsymbol{d}_n^i\} \in \Gamma^i \\
\text{min} \quad & Q_3^c = -\mathbf{f}^\mathsf{T}\mathbf{u} + \gamma_3^c R(\boldsymbol{\theta}) \\
\text{find} \quad & \boldsymbol{\theta}_3^{c*} \in \mathbb{R}^{n_e} \\
\text{s.t.} \quad & \begin{bmatrix} \mathbf{K} & -\mathbf{G}^\mathsf{T} \\ -\mathbf{G} & \mathbf{0} \end{bmatrix} \begin{bmatrix} \mathbf{u} \\ \mathbf{p} \end{bmatrix} = \begin{bmatrix} \mathbf{f} \\ \mathbf{0} \end{bmatrix} \\
& \mathbf{K}_t(\mathbf{u})\,\mathbf{T} = \mathbf{q} \\
& \sum_{e=1}^{n_e} v_e \theta_e \leq V,
\end{aligned}
\tag{38}
$$

This procedure aims to calibrate the flow balance by optimizing the diameters of pipe sections without affecting much of the geometry configurations. Eq. (25).

The topology of the conceptual design is presented in a Bitmap format file. To convert this to a CAD format file, several procedures are carried out in Grasshopper®, a graphical algorithm editor tightly integrated with Rhinoceros® 3D modeling tool. First, the interface between solid and fluid phases is captured by using *Image sampler* component, and the central lines of the pipes are found. Based on these central lines, *Pipe variable* component is used to create pipe geometries that fitted the interface. Then, a *Surface Morph* component is used to make the geometries conform to the morphological surface. To verification, the resulting geometries can be volumetric meshed and validated through three dimensional thermal-fluid simulation.

4 Numerical example

In this section, the proposed method is applied to design an optimal conformal cooling system of a core insert, which is used for manufacturing containers utilized in automated pharmacy compounding system (Fig. 5). The cylinder close to the injected part (Fig. 5 (a)) is determined as the morphological surface. Half of the cylinder surface is flattened chosen as the design domain (length: 80cm, width: 60cm). Both the inlet and outlet have a diameter of 4cm. The design of the other half of the cylinder is symmetric to the result obtained from this design domain. Two final designs are provided, namely *design A* and *design B*.

In *design A*, Dimensionless parameters are defined in design domain Ω_2^c, namely $u_0 = 1$, $p_0 = 0$, $T_0 = 0$. and heat source $q_0 = 0.01$ is uniformly distributed (Fig. 5 (a)). Further, a constant heat conductivity over the entire domain $k^0 = 10$ with $p_c = 0$ is defined. On the other hand, natural convection coefficient $h_1^0 = 0.1$ and penalty $p_n = 2$, forced convection coefficient $h_2^0 = 10$ and penalty $p_v = 2$ are determined. These setting implies, in this system, the heat transfer is mainly affected by forced convection. In addition, flow damping factor $\alpha_0 = 100$ and penalty $p_b = 0.03$ are defined. No global gradient constraint ($\gamma_2^c = 0$) is involved. Symmetric boundary condition is employed to the bottom side. The result of a thermal-fluid topology optimization is shown in Fig. 5 (b). To balance the flow, same velocities are defined in the central line, and a fluid topology optimization problem is formulated in design domain Ω_3^c, which leads the result shown in Fig. 5 (c). Then, the conceptual design is converted to a three dimensional CAD format and mapped to the morphological surface Fig. 5 (d and e). The final design is remeshed using Mimics 3-Matic®. The simulation in COMSOL Multiphysics® shows there are sufficient flow rates for entire channels and uniform fluid temperature under worst case (Fig. 6).

In *design B*, small penalties are applied by defining $p_n = 1.2$, $p_v = 1.2$ and $p_b = 1$. In addition, global gradient constraint $\gamma_2^c = 0.01$ is applied to simplify the geometry. Other parameters and boundary conditions remain the same (Fig. 7). These changes of parameters lead a result contain only one U-shape channel (Fig. 7 (b)-(d)). This simple design avoid the procedure of flow balancing, but it may results in a non-uniform temperature distribution in the fluid (Fig. 8).

The final designs are shown in Fig. 9 and 10. The cooling channels are marked in red colors. Notably, in final designs thin shells are created in order to provide additional thickness for post-process machining. Final three dimensional designs can be exported as both solid model format such as(*.x_t*, *.stp*, *.igs*, etc.), as well as surface mesh model format(*.stl*, *.vrml*, *.ply*, etc.), brings the manufacture department the convenience to run the tool path for final fitting.

5 Conclusion

In this article, a specified thermal-fluid topology optimization is introduced to optimize the conformal cooling system in an injection mold. By using this method, the traditional approaches focusing on searching for the optimal location of the pipelines is replaced to a material distribution problem. The fluid and solid phase material are optimally distributed over the entire domain in terms of their fluid and thermal-fluid properties include flow resistance, heat conduction, as well as natural and forced convection. The conceptual design is converted to a three dimensional

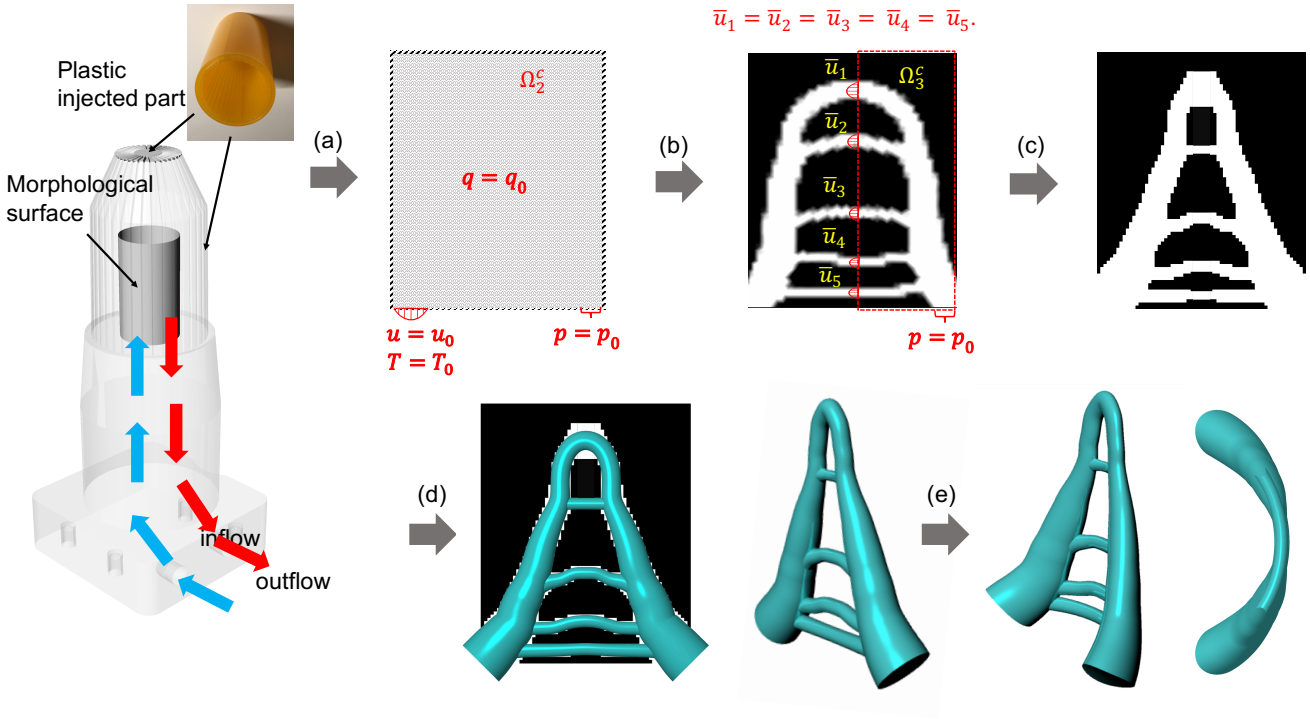

FIGURE 5. DESIGN PROCEDURE OF THE CONFORMAL COOLING SYSTEM A.

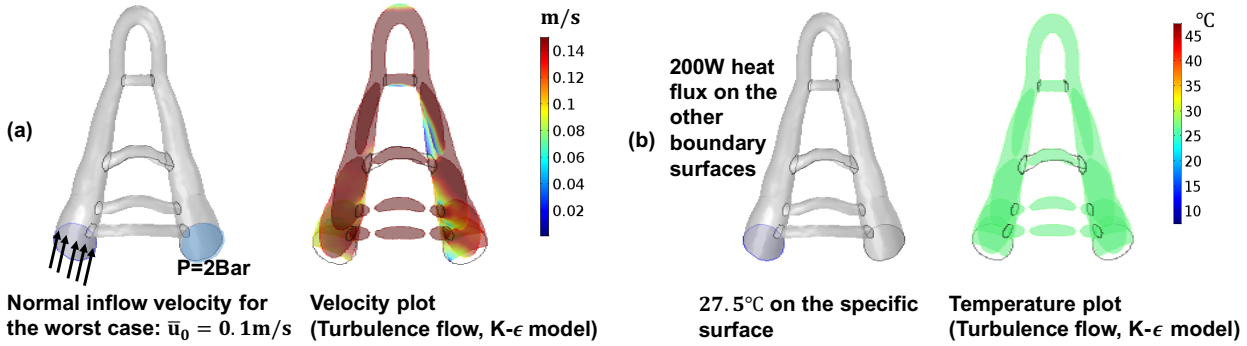

FIGURE 6. THERMAL-FLUID COUPLED SIMULATION FOR COOLING SYSTEM A.

pipe network that conformal to the injected part. The reliability of the final designs are demonstrated by simulations , and the final designs can be easily modified and produced by manufacture department.

However, several errors may occurs during the approximation. First, a Navier-Stokes equations based fluid model may lack of inertia term, resulting in a suboptimal conceptual design compared to the real case, in which the turbulent flow is employed. Second, errors may occurred while converting the two dimensional conceptual design to a three dimensional CAD format and mapping the geometry to the morphological surface. Therefore, a verification is still necessary for the design approach. The future work will focus on reduce these errors and improve the design optimality.

ACKNOWLEDGMENT

The Walmart Foundation supported this research effort. Thogus plastic injection molding company (Avon Lake, Ohio) provided the original injection mold model for the investigation.

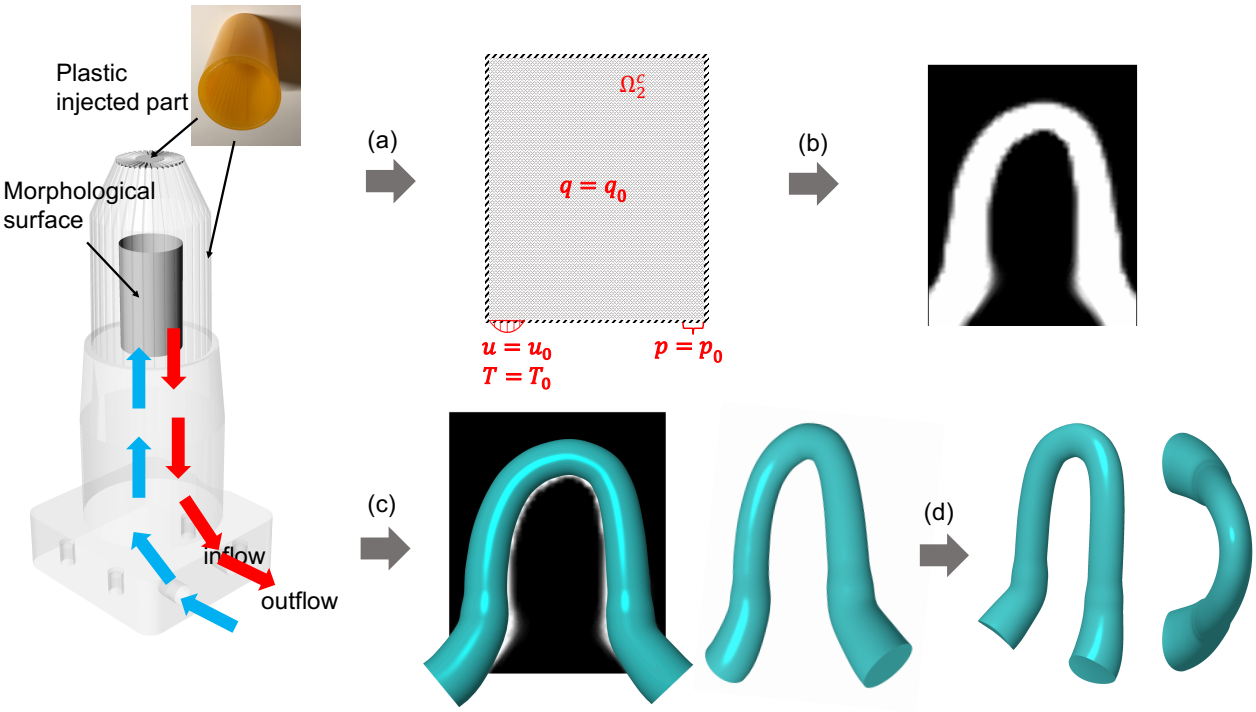

FIGURE 7. DESIGN PROCEDURE OF THE CONFORMAL COOLING SYSTEM B.

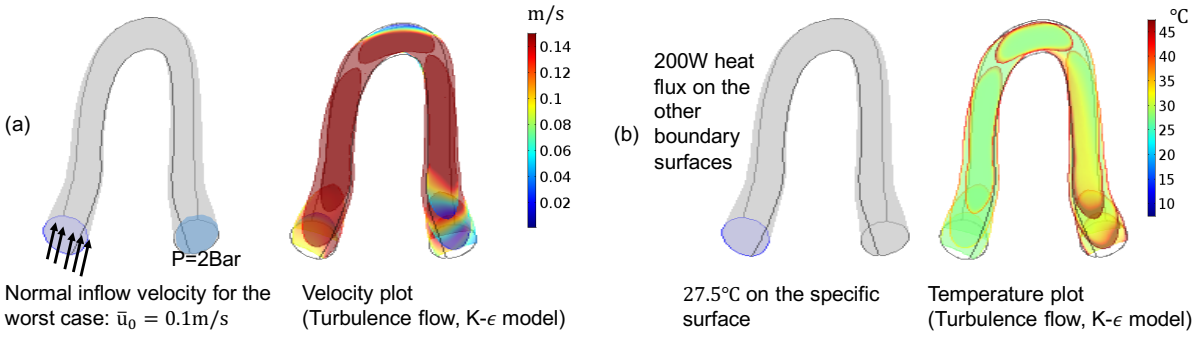

FIGURE 8. THERMAL-FLUID COUPLED SIMULATION FOR COOLING SYSTEM B.

TRUMPF Inc (Ditzingen, Germany) will 3D-printed the metal specimens. Any opinions, findings, conclusions, and recommendations expressed in this investigation are those of the writers and do not necessarily reflect the views of the sponsors.

REFERENCES

[1] Rännar, L.-E., Glad, A., and Gustafson, C.-G., 2007. "Efficient cooling with tool inserts manufactured by electron beam melting". *Rapid Prototyping Journal,* ***13***(3), pp. 128–135.

[2] Lin, J., 2002. "Optimum cooling system design of a free-form injection mold using an abductive network". *Journal of Materials Processing Technology,* ***120***(1-3), pp. 226–236.

[3] Agazzi, A., Sobotka, V., LeGoff, R., and Jarny, Y., 2013. "Optimal cooling design in injection moulding process–a new approach based on morphological surfaces". *Applied Thermal Engineering,* ***52***(1), pp. 170–178.

[4] Wang, Y., Yu, K.-M., Wang, C. C., and Zhang, Y., 2011. "Automatic design of conformal cooling circuits for rapid tooling". *Computer-Aided Design,* ***43***(8), pp. 1001–1010.

[5] Au, K., and Yu, K., 2011. "Modeling of multi-connected

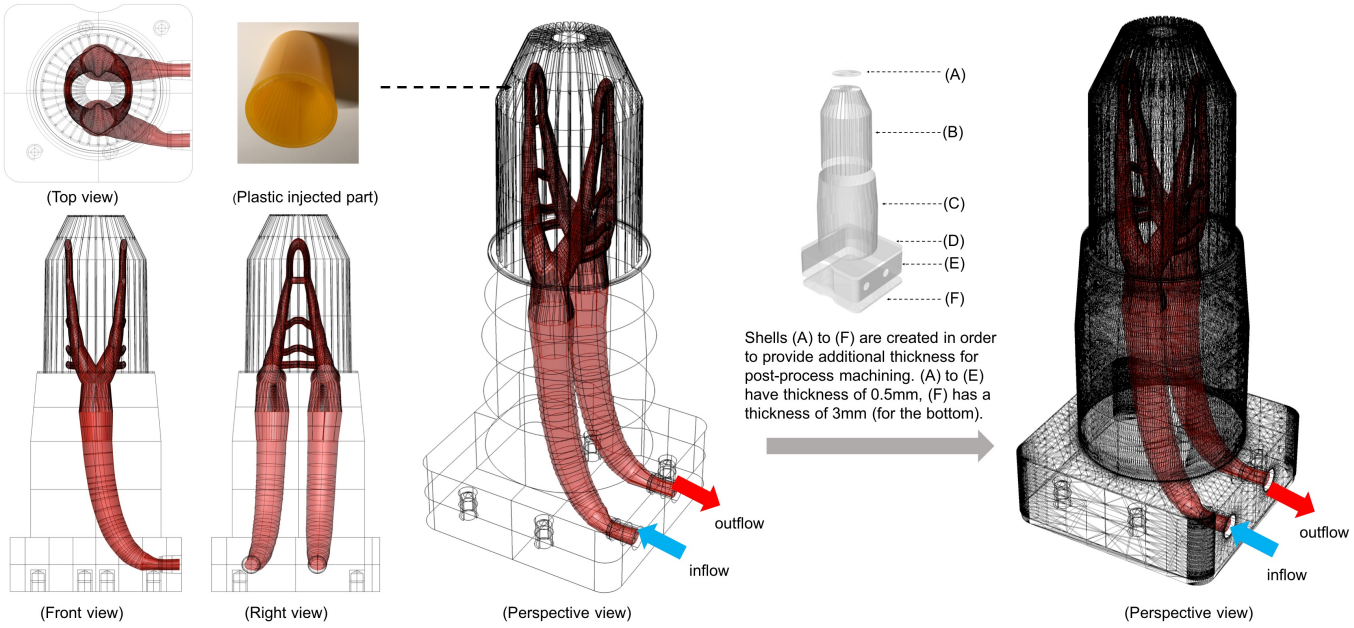

FIGURE 9. FINAL DESIGN OF *design A*

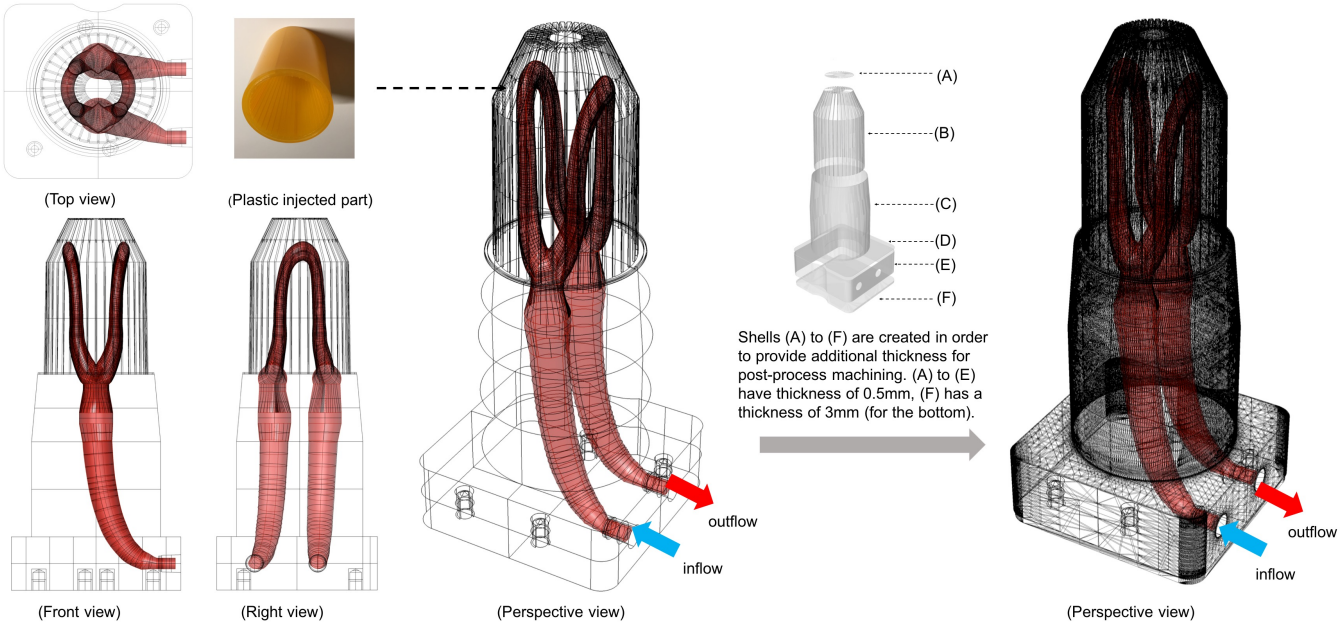

FIGURE 10. FINAL DESIGN OF *design B*.

porous passageway for mould cooling". *Computer-Aided Design,* ***43***(8), pp. 989–1000.

[6] Brooks, H., and Brigden, K., 2016. "Design of conformal cooling layers with self-supporting lattices for additively manufactured tooling". *Additive Manufacturing,* ***11***, pp. 16 – 22.

[7] Wu, T., Upadhyaya, N., Acheson, D., and Tovar, A., 2017. "Structural optimization of injection molds with lattice cooling". In ASME 2017 International Design Engineering Technical Conferences and Computers and Information in Engineering Conference, American Society of Mechanical Engineers, pp. V02BT03A008–V02BT03A008.

[8] Rao, Y., and Zang, S., 2014. "Flow and heat transfer characteristics in latticework cooling channels with dimple vortex generators". *Journal of Turbomachinery,* ***136***(2), p. 021017.

[9] Choi, J.-H., Choi, S.-H., Park, D., Park, C.-H., Rhee, B.-O., and Choi, D.-H., 2012. "Design optimization of an injection mold for minimizing temperature deviation". *International Journal of Automotive Technology,* ***13***(2), pp. 273–277.

[10] Wu, T., Jahan, S. A., Zhang, Y., Zhang, J., Elmounayri, H., and Tovar, A., 2017. "Design optimization of plastic injection tooling for additive manufacturing". *Procedia Manufacturing,* ***10***, pp. 923–934.

[11] Li, Q., Steven, G. P., Querin, O. M., and Xie, Y., 1999. "Shape and topology design for heat conduction by evolutionary structural optimization". *International Journal of Heat and Mass Transfer,* ***42***(17), pp. 3361–3371.

[12] Ha, S.-H., and Cho, S., 2005. "Topological shape optimization of heat conduction problems using level set approach". *Numerical Heat Transfer, Part B: Fundamentals,* ***48***(1), pp. 67–88.

[13] Gersborg-Hansen, A., Bendsøe, M. P., and Sigmund, O., 2006. "Topology optimization of heat conduction problems using the finite volume method". *Structural and multidisciplinary optimization,* ***31***(4), pp. 251–259.

[14] Gao, T., Zhang, W., Zhu, J., Xu, Y., and Bassir, D., 2008. "Topology optimization of heat conduction problem involving design-dependent heat load effect". *Finite Elements in Analysis and Design,* ***44***(14), pp. 805–813.

[15] Bruns, T. E., 2007. "Topology optimization of convection-dominated, steady-state heat transfer problems". *International Journal of Heat and Mass Transfer,* ***50***(15), pp. 2859–2873.

[16] Alexandersen, J., Aage, N., Andreasen, C. S., and Sigmund, O., 2014. "Topology optimisation for natural convection problems". *International Journal for Numerical Methods in Fluids,* ***76***(10), pp. 699–721.

[17] Joo, Y., Lee, I., and Kim, S. J., 2017. "Topology optimization of heat sinks in natural convection considering the effect of shape-dependent heat transfer coefficient". *International Journal of Heat and Mass Transfer,* ***109***, pp. 123–133.

[18] Dede, E. M., Joshi, S. N., and Zhou, F., 2015. "Topology optimization, additive layer manufacturing, and experimental testing of an air-cooled heat sink". *Journal of Mechanical Design,* ***137***(11), p. 111403.

[19] Alexandersen, J., Sigmund, O., and Aage, N., 2016. "Large scale three-dimensional topology optimisation of heat sinks cooled by natural convection". *International Journal of Heat and Mass Transfer,* ***100***, pp. 876–891.

[20] Iga, A., Nishiwaki, S., Izui, K., and Yoshimura, M., 2009. "Topology optimization for thermal conductors considering design-dependent effects, including heat conduction and convection". *International Journal of Heat and Mass Transfer,* ***52***(11), pp. 2721–2732.

[21] Dede, E. M., Nomura, T., and Lee, J., 2014. *Multiphysics Simulation*. Springer.

[22] Borrvall, T., and Petersson, J., 2003. "Topology optimization of fluids in stokes flow". *International journal for numerical methods in fluids,* ***41***(1), pp. 77–107.

[23] Gersborg-Hansen, A., Sigmund, O., and Haber, R. B., 2005. "Topology optimization of channel flow problems". *Structural and Multidisciplinary Optimization,* ***30***(3), pp. 181–192.

[24] Guest, J. K., and Prévost, J. H., 2006. "Topology optimization of creeping fluid flows using a darcy–stokes finite element". *International Journal for Numerical Methods in Engineering,* ***66***(3), pp. 461–484.

[25] Kreissl, S., Pingen, G., and Maute, K., 2011. "Topology optimization for unsteady flow". *International Journal for Numerical Methods in Engineering,* ***87***(13), pp. 1229–1253.

[26] Deng, Y., Liu, Z., Zhang, P., Liu, Y., and Wu, Y., 2011. "Topology optimization of unsteady incompressible navier–stokes flows". *Journal of Computational Physics,* ***230***(17), pp. 6688–6708.

[27] Yoon, G. H., 2016. "Topology optimization for turbulent flow with spalart–allmaras model". *Computer Methods in Applied Mechanics and Engineering,* ***303***, pp. 288–311.

[28] Dilgen, C. B., Dilgen, S. B., Fuhrman, D. R., Sigmund, O., and Lazarov, B. S., 2018. "Topology optimization of turbulent flows". *Computer Methods in Applied Mechanics and Engineering,* ***331***, pp. 363–393.

[29] Koga, A. A., Lopes, E. C. C., Nova, H. F. V., de Lima, C. R., and Silva, E. C. N., 2013. "Development of heat sink device by using topology optimization". *International Journal of Heat and Mass Transfer,* ***64***, pp. 759–772.

[30] Dede, E. M., 2012. "Optimization and design of a multipass branching microchannel heat sink for electronics cooling". *Journal of Electronic Packaging,* ***134***(4), p. 041001.

[31] Matsumori, T., Kondoh, T., Kawamoto, A., and Nomura, T., 2013. "Topology optimization for fluid–thermal interaction problems under constant input power". *Structural and Multidisciplinary Optimization,* ***47***(4), pp. 571–581.

[32] Yaji, K., Yamada, T., Kubo, S., Izui, K., and Nishiwaki, S., 2015. "A topology optimization method for a coupled thermal–fluid problem using level set boundary expressions". *International Journal of Heat and Mass Transfer,* ***81***, pp. 878–888.

[33] Sato, Y., Yaji, K., Izui, K., Yamada, T., and Nishiwaki, S., 2017. "An optimum design method for a thermal-fluid device incorporating multiobjective topology optimization with an adaptive weighting scheme". *Journal of Mechanical Design*.

[34] Elman, H. C., Ramage, A., and Silvester, D. J., 2007. "Algorithm 866: Ifiss, a matlab toolbox for modelling incompressible flow". *ACM Transactions on Mathematical Software (TOMS),* ***33***(2), p. 14.

[35] Svanberg, K., 1987. "The method of moving asymptotes-a new method for structural optimzation". *International Journal for Numerical Methods in Engineering,* ***24***, pp. 359–373.